Structures 67 (2024) 106922

Contents lists available at ScienceDirect

Structures

journal homepage: www.elsevier.com/locate/structures

An experimental and numerical study for local behaviour of steel-concrete composite structures with novel long-nut shear connectors

Chenguang Li [a], Jun Li [a], Xinqun Zhu [a,*], Peng Dong [b]

[a] School of Civil and Environmental Engineering, University of Technology Sydney, Ultimo, NSW 2007, Australia
[b] School of Civil Engineering, Tianjin Chengjian University, Tianjin, China

ARTICLE INFO

Keywords:
Steel-concrete composite structure
Long-nut shear connectors
Push out tests
Experimental and numerical study

ABSTRACT

An experimental and numerical study on the behaviour of the steel-concrete composite structure with the novel shear connectors has been conducted in this paper. The new bolted connector consists of a long tube nut and a compatible partial-thread bolt. The nut is casted in concrete and the bolt is connected to the nut through pre-drilled holes in the steel beam to achieve the interaction between the concrete slab and the steel beam. The push-out specimens have been designed and manufactured. The push out tests are carried out to investigate the stiffness, strength, and ductility of the new connectors in concrete and the results are compared with that using conventional welded connectors. A finite element model is established and validated using experimental results. With the validated finite element models, the effect of the concrete strength, the shear connector diameter, the bolt pretension, the gap between the bolt hole and bolt, and the nut diameter on the local behaviour of shear connectors are analysed and discussed. The results show that the novel bolted shear connectors have superior ultimate load capacity and ductility compared to conventional welded connectors. This novel bolt connection could also achieve the equal shear resistance in all directions and reduce the stress concentration in the tangible medium.

1. Introduction

The steel-concrete composite structure is widely used for building and bridge constructions as it makes full use of the resistance of the concrete and steel components against compression and tension [1,2]. To ensure the steel and concrete work together effectively, shear connectors are used at the steel-concrete interface to transfer the longitudinal shear and prevent the separation between these two components [3,4]. The headed studs are widely used for conventional steel-concrete composite structural systems. These studs are welded to the top flange of the steel beam and embedded in the cast in-situ concrete slab. It is difficult to deconstruct and reuse the building components in conventional steel-concrete composite structures as the studs are fully embedded in concrete and welded to the steel beam. A large amount of waste would be generated when the structure is dismantled after its service life [5]. The repair of a deteriorated bridge deck is also a cost and time-consuming process involving concrete crushing and drilling [6]. To meet the modern sustainability targets, it is crucial to develop demountable shear connectors for recycling/reusing the structural components at the end of the service life [7].

The bolted shear connectors allow for the easy deconstruction of the steel-concrete composite structures at the end of their service life and the fast replacement of a deteriorated composite bridge deck [8,9]. The bolts are installed in pre-drilled holes in the steel flanges to transfer the shear at the interface between the slab and the steel sections. It easily connects the existing steel beam with concrete slab and allows them to work together effectively. The flexural behaviour of steel-concrete composite beams with two types of blind bolted connectors have been investigated experimentally and numerically and the results are compared with that by conventional welded stud connectors [10,11]. The results show that bolted connectors have a higher slip capacity and the larger slip displacement during shear transformation without yielding compared with conventional stud connectors. Due to the sustainability advantages, the high installation efficiency, and superior mechanical properties of bolted shear connectors, various types of bolted connections have been employed in composite structures in last two decades. The bolt without embedded nut was first studied by Hawkins [12] as a shear connection in composite beams. The experimental results indicated that, in comparison to conventional connectors, these bolted shear connectors enhanced the ductility of the structure. However, there

* Corresponding author.
E-mail address: xinqun.zhu@uts.edu.au (X. Zhu).

https://doi.org/10.1016/j.istruc.2024.106922
Received 15 February 2024; Received in revised form 17 June 2024; Accepted 13 July 2024
Available online 24 July 2024

was a reduction in both the slip capacity and shear stiffness of the structure. Pavlović et al. [13] used push-out experiments to study the slip behaviour of composite beams with different types of connectors. Their findings indicated that a bolted shear connector employing a single nut exhibited superior resistance to slippage when compared to conventional welded shear studs. Additionally, they emphasized that the nut played a pivotal role in influencing both the ultimate slip capacity and shear stiffness of the connection. Kwon et al. [14] conducted a series of experiments to investigate the mechanical behaviour of a bolt with double embedded nut under static and fatigue loading conditions. The experimental results indicated that the double embedded nut exhibited excellent stiffness and strength under the two different loading conditions due to the increased contact area between the connection and the concrete, which retarded the crushing of the concrete.

From the above study, it can be observed that increasing the surface area of nuts embedded within concrete slabs can reduce the concentration of forces leading to longitudinal cracking in the concrete slabs, thereby enhancing the structural mechanical performance. Tzouka et al. [15] presented a special locking nut configuration to prevent the slip of the bolts within their holes. Suwaed et al. [5] and He et al. [16,17] employed a numerical and experimental study for the mechanical characteristics of structures incorporating removable welded connections utilizing long tube nuts. Their findings indicated that the long tube nut reduced the stress concentration in the concrete near the connector, which delayed the cracking of the concrete and enhanced the shear resistance of the structure. However, in the practical engineering, the application of these connectors requires specialized equipment and skilled workers to weld the studs to the steel beams and fill the connectors with concrete mortar. This complexity leads to an inefficient construction process.

To address these challenges, this paper proposes an innovative bolt shear connector that combines the advantages of traditional bolt-type connectors and long tube nuts. This novel connection consists of a long tube nut and a compatible partial-thread bolt. The tube nut is selected to provide equal shear resistance in all directions and reduced the stress concentration in the tangible medium compared with traditional studs. The local behavior of this new connection is investigated using push-out tests and the results are compared with that of conventional welded connectors. The load-slip curves from experimental results are used to evaluate the performance of shear connectors including the shear stiffness, ultimate strength, and ductility of the structure. A nonlinear finite element model is established and validated against the experimental results. Parametric study is then carried out on the effect of the bolt size, concrete strength, nut diameter, bolt pretension, and the diameter of the prefabricated holes in composite structures. The results show that the novel bolted shear connectors have superior ultimate load capacity and ductility compared to conventional welded connectors.

2. Description of the long-nut shear connector

The novel bolt shear connection consists of three components: a tube nut, a washer, and a bolt, as shown in Fig. 1. The tube nut is with a height of 70 mm, an inner diameter of 20 mm, and an outer diameter of 30 mm. The bolt is of M20 grade 8.8 high-strength classification. Fig. 1(a) shows the assembly of the shear connection system, that the connection is established through pre-drilled holes on the steel beam, and embedded nuts within the concrete. Fig. 1(b) lists the detail dimensions of the long tube nut. Fig. 1(c) presents the details of the innovative connectors in 3D view and the connection to the steel girder flange.

3. Experiment study

According to Eurocode 4 [18] (British Standards Institution, 2004), two sets of push-out specimens have been designed and manufactured in the laboratory. Two of them are with novel bolted connections and another two are with welded studs as comparison. The push out testing has been conducted to investigate the local connection behaviour of novel shear connectors and the results are compared with that by welded

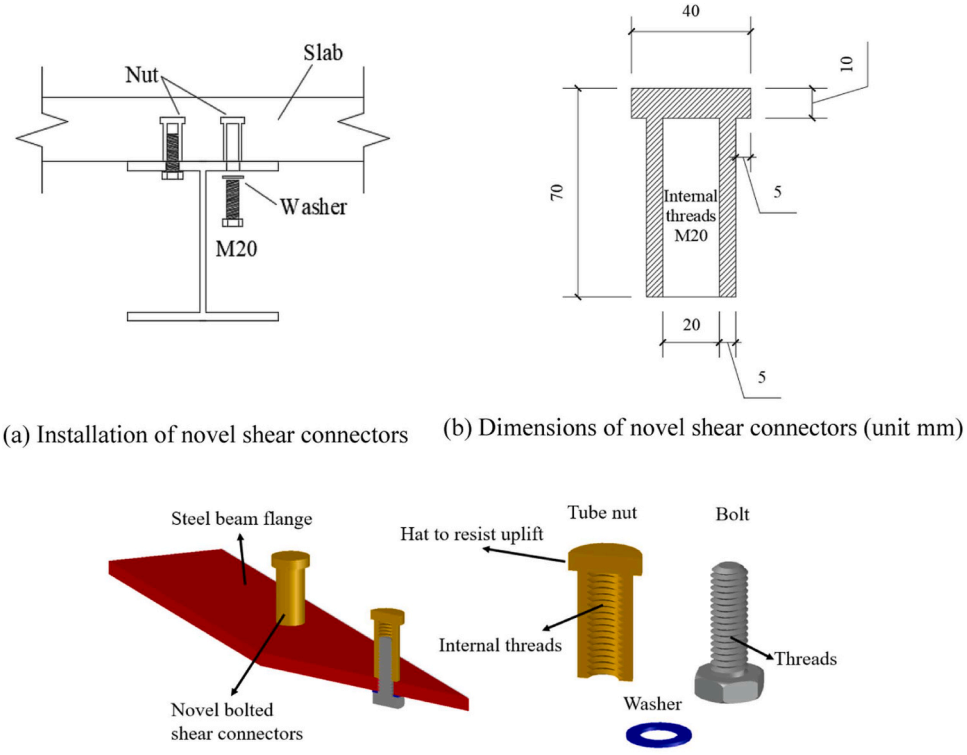

Fig. 1. The novel shear connection system.

connectors. The detailed description of the model preparation and installation, experimental setup and results is listed in Section 3.1. The experimental results will be used to validate the finite element model in Section 4.

3.1. Specimen preparation

The designed specimen is shown in Fig. 2, and the dimensions of all constituent components are listed in Table 1. The steel sections were prefabricated at a manufacturer, and the concrete slabs were meticulously prepared following the stipulated guidelines provided by the manufacturer. The concrete material testing was carried out. At the lapse of five days, the compressive strength of the concrete cubes had attained 50 % of its peak magnitude, proving that the strength of the concrete material was compliant with the design requirements [19] (Ministry of Housing and Urban-Rural Development of China, 2019). Additionally, steel bars with a diameter of 10 mm were embedded in the concrete slab. There were two types of connectors, namely traditional welded studs, and the novel bolt connectors. The welded studs, affixed to the steel beam prior to concrete deposition, possessed a diameter of 19 mm and featured a 10 mm-high, 20 mm-diameter cap. On the other hand, the bolted shear connectors included three components: a long tube nut, a washer and a compatible partial-thread bolt. The nut was embedded in the concrete slab, and the bolts were of M20 8.8 grade, which were connected with the nut through the pre-drilled holes on the steel beam to achieve the interaction between the concrete slab and the steel beam. A torque wrench was used to add the pretension to the bolt. The value of the pretension was 98 kN. The installation of the two connectors and the steel beam was listed in Fig. 3. Concrete was poured in the wooden formwork and cured for 28 days.

Table 1
The dimensions of all components.

Component	Dimensions
Concrete slabs (mm)	600 * 150 * 650
Steel beam flange (mm)	250 * 14 * 650
Steel beam webs (mm)	222 * 9 * 650
Height of connections (mm)	70
Diameter of reinforcement (mm)	10

3.2. Experiment setup

Fig. 4(a) illustrated the push-out testing setup. Four LVDTs were installed for each specimen to measure the interfacial slip occurring between the concrete slab and the steel beam. The configuration of the LVDTs was presented in Fig. 4(b). Two LVDTs were affixed to the frontal

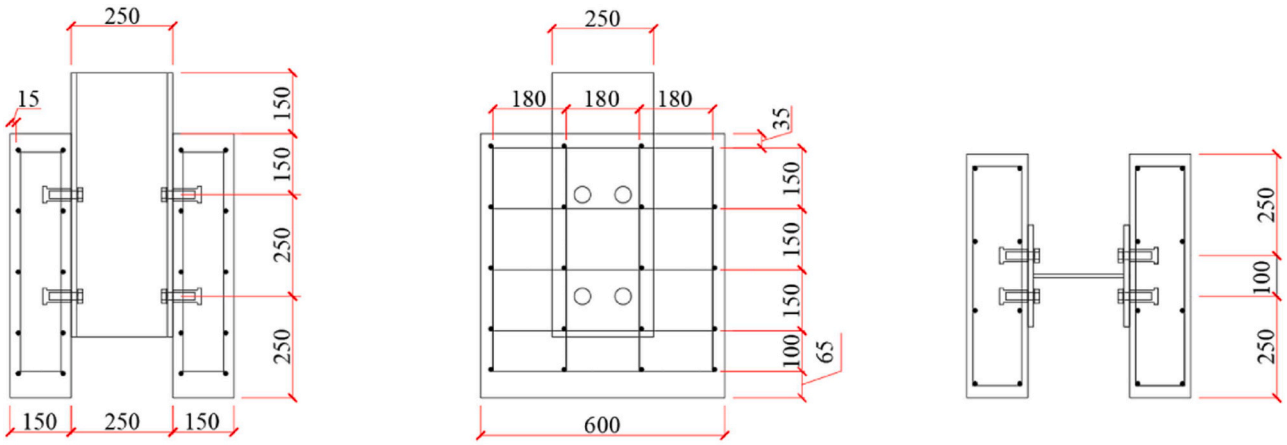

(a) The specimen with novel bolted shear connectors

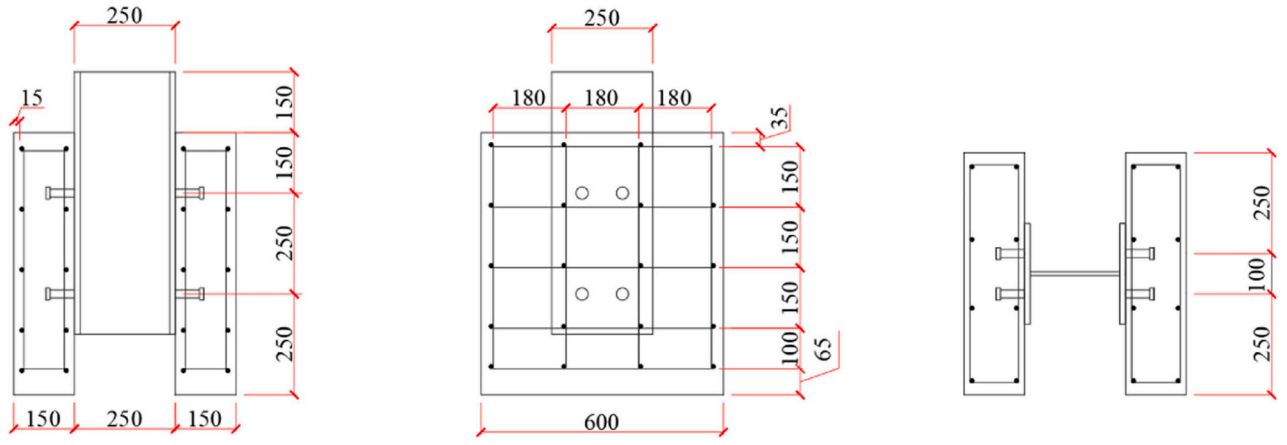

(b) The specimen with welded studs

Fig. 2. The specimens with different shear connectors (unit mm).

Fig. 3. Installation of the shear connection.

aspect of the structure, while the other two LVDTs were situated on its posterior side. Each individual LVDT was installed near the connectors. To mitigate the impact of horizontal friction during the experiment, a layer of fine sand was interposed between the underside of the concrete slab and the supporting surface. The load was applied at the top of the steel beam. According to Eurocode 4 [18] (British Standards Institution, 2004), a preload was applied to the model. This preload was cycled 25 times with values ranging from 5 % to 40 % of the theoretical failure load. Then, the experimental specimen was subjected to a displacement load of 0.15 mm/s until the load dropped to 20 % of the maximum load. Failure loads for all specimens were calculated in accordance with the load carrying capacity of welded studs provided in GB/T50017-2017 [20] (Ministry of Housing and Urban-Rural Development of China, 2017). The theoretical calculated ultimate load of the connector was calculated according to Eq. (1).

$$N_v^c = 0.43A_s\sqrt{E_c f_c} \le 0.7A_s\gamma f \quad (1)$$

where, E_c is the elastic modulus of concrete (N/mm^2); A_s is the cross-section area of stud (mm^2); f_c is the concrete compressive strength (N/mm^2); f is the value of the tensile strength of the stud (N/mm^2); γ is the ratio of the minimum tensile strength to the yield strength of the stud material. The theoretical calculated ultimate loads and experimental results for all specimens are detailed in Table 2.

3.3. Experimental results

To compare the mechanical properties of the new bolted connectors with those of the conventional welded studs, the load-slip curves of the specimens with different connections are shown in Fig. 5. From Fig. 5, the load slip curve for new bolted connectors can be divided into four phases after the preloading has been completed. In the initial phase, the load ascends from 0 to 400 kN. During this phase, the shear force between the concrete slab and the steel beam predominantly with the

Table 2
Experimental and estimated results of specimens.

	Welded studs	Novel bolted connectors
Theoretical calculated ultimate load (kN)	835.29	835.29
Experimental measured ultimate load (kN)	850.05	1243.09
Stiffness of shear connector (kN/mm)	145.52	156.14
slip capacity (mm)	8.86	13.31
Predicted failure modes	Concrete crush	Concrete crush
Failure modes	Concrete crush	Concrete crush

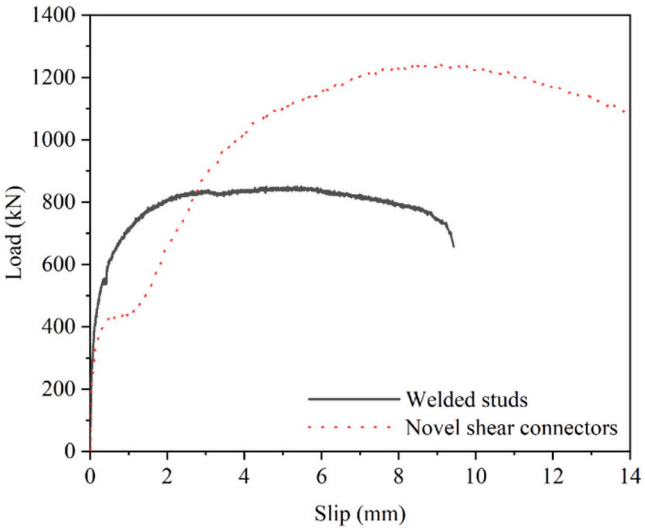

Fig. 5. Load-slip behaviour of the specimens with different shear connections.

Fig. 4. Experimental setup.

resistance through the static friction. The second phase begins with an abrupt change in the slip between the concrete slab and the steel beam upon reaching a load of 400 kN. This is due to the gap between the bolt and its hole after the specimen installation. It is noted that the value of the slip is inherently uncertain due to the stochastic nature of the gaps between the bolts and their corresponding holes. Transitioning to the third phase, the load continues to increase until reaching its maximum value. Within this phase, fine cracks emerge in proximity to the connections. The final phase corresponds to the plastic regime of the structure with the concrete deformation and consequent crushing. Then, the structural load reduces as the slip continues increasing. In contrast, the load-slip curve for the conventional welded studs exhibits a tripartite progression. The initial stage, encompassing a load range of 0 to 480 kN, manifests a linear increase in the load-slip correlation, signifying the elastic regime. Upon the attainment of a 480 kN load, the second phase unfolds, marked by the emergence of fractures at the interface between the concrete slab and the steel beam. Concurrently, the incremental rise in load progressively diminishes with the increasing slip. The ultimate stage of this specimen is characterized by reaching its maximum load-bearing capacity, followed by a decline in load magnitude as slip increases.

The load carrying capacity of the connection corresponds to the peak load in the load-slip curve detailed in Table 2. From Fig. 5, in terms of ultimate load capacity, that of the new bolted shear connectors is much larger than that of conventional welded studs. There is an 46.23 % increment in the ultimate load in comparison to the conventional shear connector. According to Eurocode 4 [18] (British Standards Institution, 2004), the slip capacity is a parameter designated for delineating the ductility attributes of connections, and it is defined as the degree of slip corresponding to a load reduction to 10 % of the peak load within the plastic phase. From Fig. 5, the slip load capacity of the new bolt connector is 1.5 times greater than that of conventional welded studs. The long tube nut reduces the concentrated stresses in the concrete due to the large contact area with the concrete and this protects the concrete from cracking resulting in a higher load capacity and ductility compared to conventional shear connectors. The similar results are also found in the reference by Suwaed et al. [5].

According to Eurocode 4 [18] (British Standards Institution, 2004), The shear stiffness for the connection is throughout the push-out test is obtained as,

$$k = \frac{0.7P_{Rk}}{s} \tag{2}$$

where P_{Rk} is 90 % of the ultimate load (kN). s is the slip when the load reaches $0.7P_{Rk}$ (mm).

By Eq. (2), the results of shear stiffness are listed in Table 2. From Table 2, the shear stiffness of the new bolted connection is 7 % higher than that of the conventional connection. Moreover, the shear stiffness of the bolted shear connector exhibits a complicated profile due to the presence of bolt clearance hole. As shown in Fig. 5, the load-slip relationship curve can mainly be divided into three stages. In the first stage, the load is resisted by the friction between the concrete slab and the steel beam, and the shear stiffness of the novel shear connection is approximate the same as that of the conventional welded studs. In the second stage, the friction is overcome at a load value of 400 kN, and there is a slip between the concrete slab and the steel beam in the novel shear connection due to the bolt clearance. Consequently, the stiffness of the novel shear connection is lower than that of the welded studs in this stage. In the third stage, the bolt gap is eliminated. The contact between the bolt and the bolt hole occurs, which results in a high stiffness of the novel connection specimen. The overall shear stiffness of the new bolted connection is greater than that of the conventional welded connection.

Fig. 6 shows the failure modes of the specimens with different shear connectors. Fig. 6(a) shows the failure mode of the specimens with welded studs and Fig. 6(b) shows the failure mode of the specimens with novel shear connectors. From Figs. 6(a) and 6(b), the specimens with different shear connectors have the similar failure pattern, e.g. concrete crushing, with initial crack occurring close to the connection points.

(a) The specimen with welded studs (b) The specimen with novel shear connectors

Fig. 6. Failure modes.

4. Finite element model

A 3D non-linear finite element model was established using Abaqus in this section. For the FE model, all components were built using solid elements except for the reinforcement. The finite element (FE) model was validated using experimental results in Section 3. Then the parametric study was carried out using the validated model.

4.1. Material properties

Mechanical properties of materials were acquired through material tests in accordance with GB/T 50081–2019 [19]. Concrete's material testing is to obtain its ultimate strength and modulus of elasticity. The ultimate compressive strength was evaluated using three 100 mm cubes, with the average value of the compressive strengths derived from these specimens being considered as the resultant value. The determination of the elastic modulus involved six prismatic specimens sized at 100 * 100 * 300 mm. The calculation of the elastic modulus is based on GB/T 50081–2019 [19], with the average value of the computed results being taken as the elastic modulus of the concrete. The modulus of elasticity and ultimate compressive strength of concrete were calculated to be 32,184.67 MPa and 26.8 MPa, respectively. Regarding the reinforcement steel and shear connectors, a series of tensile tests were conducted to obtain the yield and ultimate strength of the steel. The steel properties for different steel components were listed in Table 3.

4.1.1. Concrete properties

To establish the finite element model, the elasticity and plasticity inherent to both concrete and steel were adequately considered. The incorporation of concrete's plastic behaviour was realized through the utilization of the concrete plastic damage option in Abaqus. In the Concrete Damage Plasticity (CDP) model, the required plasticity

Table 3
Steel properties for different steel components.

	Yield strength (MPa)	Ultimate strength (MPa)
Bolts	680	800
Studs	590	630
Nut	809.22	937.36
Steel beam	376.70	567.80
Bars	345.10	498.23

parameters included flow potential eccentricity, dilation angles, the ratio of biaxial to uniaxial compressive strength, the ratio of the second stress invariant on the tensile meridian to that on the compressive meridian, and the viscosity coefficient. These parameters were set as 0.1, 30 degrees, 1.16, 0.6667, and 0.001, [21] respectively.

The compressive plastic behaviour and the tensile plastic behaviour of concrete were defined separately. The description of the mechanical behaviour of the concrete under compression follows GB/T 50010-2015 [22] (Ministry of Housing and Urban-Rural Development of China, 2015), and the stress-strain relationship from elastic to plastic stages is defined below.

$$\sigma_c = (1 - d_c)E_c\varepsilon_c \tag{3}$$

$$d_c = \begin{cases} 1 - \dfrac{\rho_c n}{n - 1 + x^n} & x \le 1 \\ 1 - \dfrac{\rho_c}{\alpha_c(x-1)^2 + x} & x > 1 \end{cases} \tag{4}$$

$$\rho_c = \frac{f_{c,r}}{E_c\varepsilon_{c,r}} \tag{5}$$

$$n = \frac{E_c\varepsilon_{c,r}}{E_c\varepsilon_{c,r} - f_{c,r}} \tag{6}$$

$$x = \frac{\varepsilon_c}{\varepsilon_{c,r}} \tag{7}$$

where $f_{c,r}$ is the uniaxial characteristic compressive strength of concrete (MPa), σ_c and ε_c are the uniaxial compressive stress and strain of concrete, respectively. $\varepsilon_{c,r}$ is the strain corresponding to the peak value of the test stress-strain curve of the concrete material. α_c is a factor about the descending portion of the uniaxial compressive stress-strain curve of concrete. The values of $\varepsilon_{c,r}$ and α_c can be found in the GB/T 50010-2015 [22] (Ministry of Housing and Urban-Rural Development of China, 2015). When the concrete is in tension, it is assumed that the concrete would crack and lose its bearing capacity after reaching the maximum tensile strength, and the relationship between stress and strain is simplified as linear. In addition, the uniaxial ultimate compressive stress is 10 times larger than the uniaxial ultimate tensile stress [23]. The damage factor in the CDP model is introduced to describe the stiffness degradation parameters of concrete under cyclic loading. The damage factor of concrete is expressed as [24,25],

$$d = 1 - \sqrt{\frac{\sigma_c}{E_0\varepsilon_c}} \tag{8}$$

where E_0 is the initial elastic modulus of the concrete. σ_c and ε_c are the stress and strain of the concrete respectively. The specific compressive behaviours and compressive damage parameters versus cracking strain curves for concrete are detailed in Fig. 7.

4.1.2. Steel

According to GB 50010-2015 [22] (Ministry of Housing and Urban-Rural Development of China, 2015), the stress-strain relationship for steel was characterized using a simplified linear model [25,26]. The constitutive relation of steel was simplified into two stages, namely elastic and plastic stages as shown in Fig. 8. The strain at the initiation of strain hardening ε_{st} and the ultimate strain limit ε_{su} were presumed to be 0.02 and 0.25, respectively. In the FE model, ε_{f1} represents the fracture strain. This parameter was defined as 0.2.

4.2. Finite element model meshing

All components, except for the reinforcement, were constructed using 3D elements. The structure was first modelled using CAD and then imported into Abaqus with its original dimensions. The finite element mesh was shown in detail in Fig. 9. The specimens for the push out experiments were symmetrical about the concrete slab centreline and the steel beam web centreline. To save computational costs, a quarter of the structure was chosen for the simulation.

The steel reinforcement embedded within the concrete was represented using two-node linear truss elements (T3D2). The concrete slab, steel beam, and connectors were modelled utilizing eight-node hexahedral linear reduction integral elements (C3D8R). To optimize computational efficiency without compromising the precision of the results, a mesh convergence test was conducted. Adequate meshing constitutes a pivotal aspect of numerical simulations when employing finite element software. A FE model featuring bolted shear connection was utilized as an illustrative case for mesh sensitivity analysis. This involved the assessment of three distinct mesh configurations for the FE model, as comprehensively outlined within Table 4.

The stress distribution exhibited a high degree of complexity in the proximity of the bolt holes, necessitating a heightened mesh density in this region. The outcomes of the sensitivity analysis conducted for each component of the FE model are depicted in Fig. 10. From the figure, the numerical results were different when the mesh size varied. Compared with the experimental result, the discrepancies for Configurations 1, 2 and 3 were 1.48 % 0.37 % and 1.95 % respectively. The results showed that the accuracy of Configuration 2 was superior to that of Configurations 1 and 3. In terms of computational efficiency, the calculation time required for Configuration 2 was a mere one-fourth of that demanded by Configuration 3. Consequently, Configuration 2 was adopted as the preferred meshing method for the FE model. It was also considered that

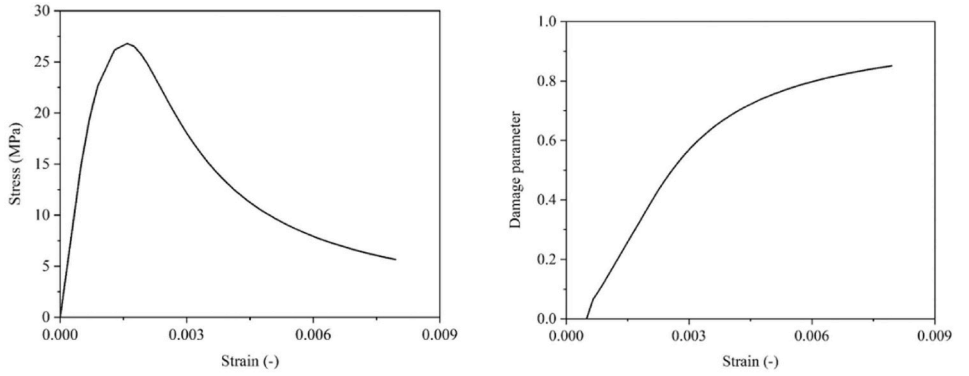

(a) Stress–strain relationship of concrete in compression (b) Compression damage of concrete

Fig. 7. Concrete compressive behaviour.

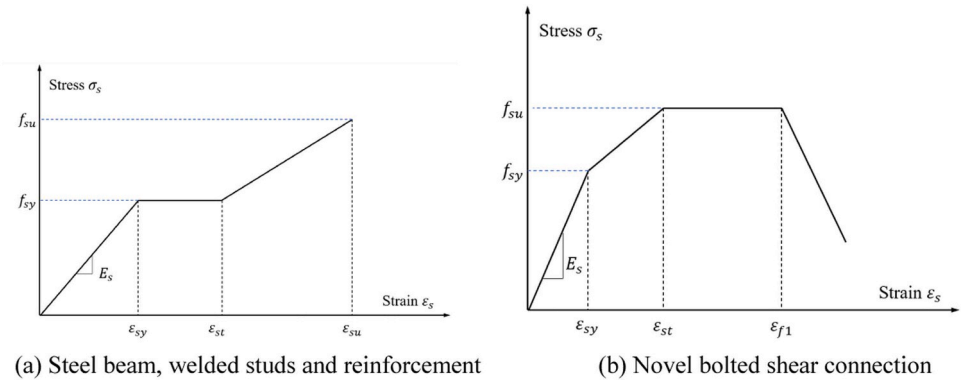

(a) Steel beam, welded studs and reinforcement (b) Novel bolted shear connection

Fig. 8. Stress–strain relationship for steel.

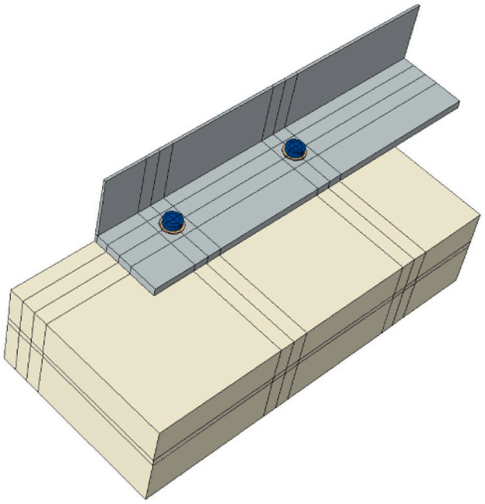

Fig. 9. Finite element model of push out test specimen.

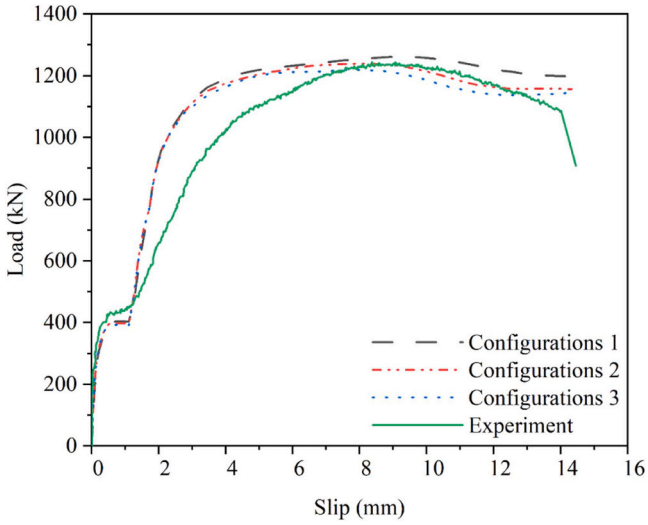

Fig. 10. Mesh convergence analysis of the FE model.

Table 4
Mesh configuration for FE models.

	Configuration 1	Configuration 2	Configuration 3
Concrete slab	7.5-30 mm	5-20 mm	2.5-10 mm
Steel beam	7.5-15 mm	5-15 mm	2.5-15 mm
Shear connectors	7.5 mm	5 mm	2.5 mm
Calculation time	0.5 h	3 h	12 h
Ultimate strength	1261.53 kN	1238.43 kN	1218.87 kN

the mesh sizes of the contact surfaces should be consistent with each other. Therefore, the meshing configurations for the concrete slab, the steel beam and the connectors were 5–20 mm, 15 mm and 5 mm respectively and the results for the FE model detailed in Fig. 11.

4.3. Interactions and boundary conditions

The interaction between various components of the FE model was characterized by utilizing two distinct options provided within Abaqus, namely "interaction" and "constraint." In accordance with the experimental results in Section 3, which indicated the absence of slippage between the root of the welded studs and the steel beam, the contact interaction between these elements was established as a "tie" constraint. To reduce the computational cost, the slip between the steel and concrete was ignored in the FE model and the contact was defined as the “embedded” in the constraint option. In addition, the interaction option was applied to the contact among the rest parts of the specimen. In the contact property, the tangential and normal behaviours of the interaction among different contact surfaces were defined as "Penalty" and "Hard". The coefficients of friction were determined as 0.4 for the concrete-steel interface and 0.25 for steel-steel contact. In the selection of the contact, since the general contact used of finite sliding discrete method, this was the same as the method of setting the contact pair. The general contact algorithm used a penalty function calculation method and a strain-free adjustment method to eliminate over-constraints. The setting of this contact mode made the calculation process more efficient. The interactions between the different parts of the model were shown in Table 5.

The FE model was one-fourth of the original model. When considering the boundary condition of the FE model, there were two aspects to be considered, one was the boundary constraint of the symmetry plane, and the other was the model support constraint.

Fig. 12 shows the boundary surfaces and the model exhibited symmetry along two distinct directions. Firstly, the plane of symmetry aligned with the centre of the steel beam web, thereby mandating the restraint of Surface 1’s movement in the x-direction, as well as precluding rotation about the y and z axes. Secondly, due to the symmetry encompassing the steel beam flange and the centre of the concrete slab, it became imperative to constrain all nodes residing on Surface 2 from movement in the z-direction and rotations about the x and y axes. Considering the practical boundary conditions of the push-out experiment, all nodes on the support surfaces were constrained from moving in the Y direction to resist compressive loads.

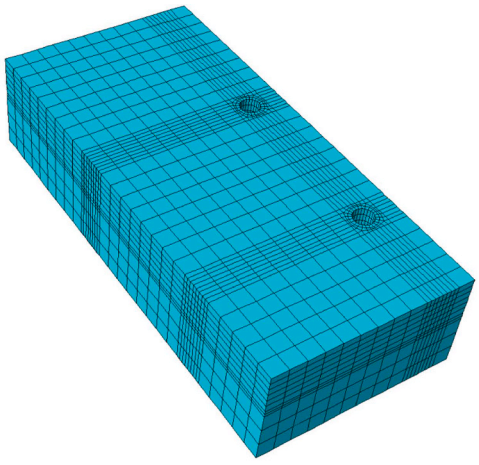

(a) Concrete slab

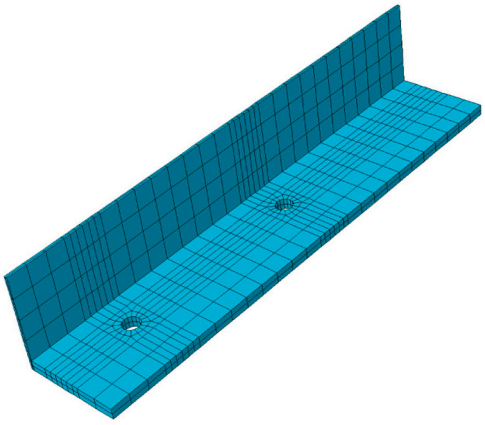

(b) Steel beam

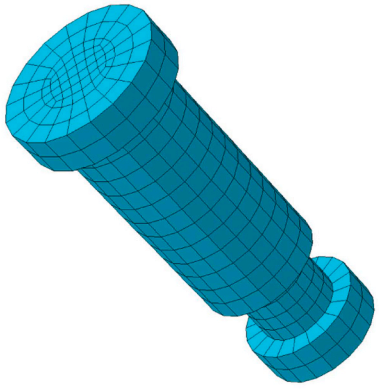

(c) Novel shear connector

Fig. 11. Finite Element Model Meshing.

4.4. Analysis procedure

As shown in Fig. 12, a displacement action was enforced at the upper portion of the steel beam in the FE model, aligning with the loading point in the experimental setup. The FE model encompassed a series of analytical steps. The first step was to establish the interaction contacts within the model, and they were designed to enhance computational efficiency. In the second step, the pretension force was added to the bolts. The magnitude of the bolt's pretension was set at 98 kN and the bolt pretension force was the same as that in the experimental testing. It's worth noting that this pretension was added using a torque wrench in the tests. In the third step, the bolt's length was maintained as a constant when the bolt was loaded. The length was limited to retain the initial length in this step. That means the bolt's length would not change under subsequent external load application. The displacement action was imposed at the designated location in the model. The relationship between the experimental load and the displacement action was extrapolated from the reaction force observed at the support.

Table 5
Contact interaction between parts of beam models.

Part instance		Contact type
Concrete slab	Steel beam	Interaction
Concrete slab	Nut	Interaction
Bolt	Nut	Tie
Bolt	Beam	Interaction
Nut	Beam	Interaction
Welded studs	Concrete slab	Interaction
Welded studs	Beam	Tie
Reinforcement	Concrete slab	embedded

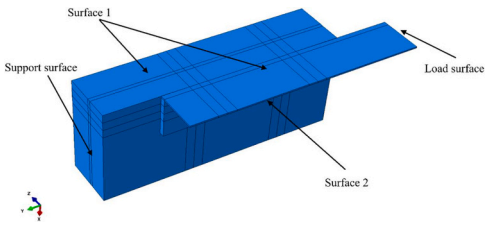

Fig. 12. Definition of boundary surfaces.

4.5. Model validation

To validate the FE model, the results of the numerical model were compared with experimental results. Fig. 13 showed the numerical and experimental results of specimens with conventional welded studs and new bolt shear connectors. From Fig. 13, the results of the FE model for the conventional welded studs were agreed well with the corresponding experimental results, especially the initial stiffness and ultimate

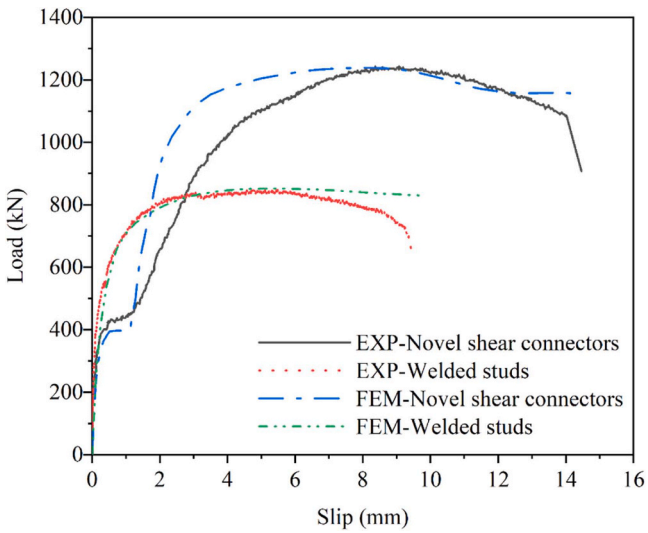

Fig. 13. FE Model validation.

strength. For the new bolted shear connectors, the load-slip curves of the FE model are also close to the corresponding experimental results. There is a changing point in Fig. 13 when the load attains the magnitude of 450 kN. The changing point is related to a slip displacement due to the gap between the bolt and its bolt hole when the load overcomes the frictional resistance. After the establishment of contacts among these components, the bolt takes its crucial role to resist the shear forces, and there is a transformative shift in the FE model's stiffness. Notwithstanding this coherence, a slight divergence emerges, noticeable when the load surpasses 480 kN. This discrepancy in stiffness is rooted in the experimental specimens' inherent defects and the non-idealized nature of their boundary conditions. Nevertheless, this divergence, while noteworthy, remains within reasonable bounds and mirrors the identical trend observed post-peak. Fig. 14 shows the failure patterns of specimens and they are concrete deterioration. From Fig. 14, the failure patterns are similar to that observed in the experimental tests. As the above, it could be concluded that the FE model is validated, and it will be used predict the mechanical behaviour of the specimen in the push out experiment in Section 4.6.

4.6. Parametric studies

A series of parametric analyses were carried out in this section. The influence of the size of the prefabricated bolt holes, the pretension of the bolts and the diameter of the nut and screw on the structure would be discussed. The effects of the concrete strength on the conventional welded studs and the new bolted shear connector were also compared.

4.6.1. Effect of the size of the prefabricated hole on steel beams

To improve the efficiency of the installation, the bolt holes in the steel beams were pre-drilled at the location of the connections. The diameter of the pre-drilled holes was often larger than the diameter of the bolts considering the tolerance and manufacturing errors. So there was a gap between the bolts and the pre-drilled holes in the steel beam. From experimental results in Section 3, this clearance affected the mechanical behaviour of the bolted connection. To investigate the influence of the bolt holes in the steel beam on the structure, the parametric analysis was carried out with four different bolt hole diameters, e.g. 22 mm, 24 mm, 26 mm, and 28 mm. Fig. 15 and Table 6 showed numerical results of push out tests with different diameters of prefabricated holes. It was assumed that the position of the bolt was at the centre of the bolt hole before the loading was added. The numerical results showed that the load capacity of the innovative shear connector was not affected by the hole diameter from 22 mm to 28 mm. The load deflection curves of different specimens were approximate the same in the elastic phase up to the first critical point. Due to the different clearances between the bolt holes and the bolts, the corresponding slip displacements of the structure were different after the frictional forces were overcome. The larger the bolt hole diameter was, the greater the slip was when the bolt was in contact with the edge of the bolt hole. This trend was the same as the results obtained by Liu et al. [27].

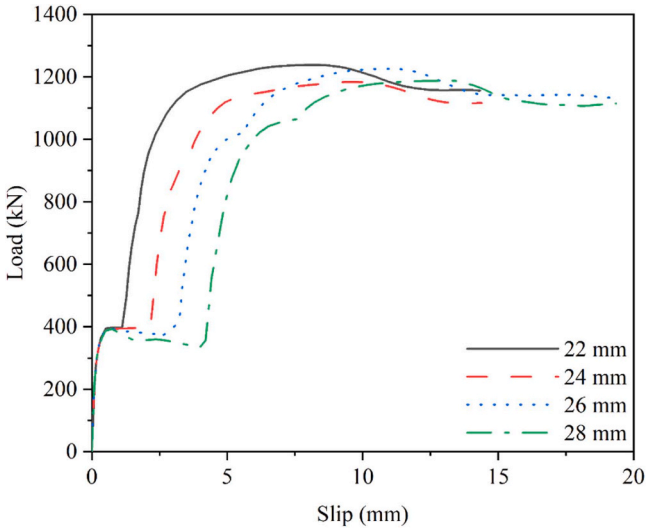

Fig. 15. Effect of diameter of bolt gap for novel bolted shear connectors.

Table 6
Effect of the diameter of the bolt gap for novel bolted shear connectors.

Dimensions of prefabricated holes (mm)	Ultimate load (kN)	Stiffness of shear connector k (kN/mm)
22	1238.43	232.00
24	1184.24	233.49
26	1225.85	232.64
28	1188.30	230.17

4.6.2. Effect of pretension of bolts

The incorporation of bolted shear connectors inherently necessitates the application of preload to the bolts during installation. Optimal bolt pretension serves two purposes: enhancing the joint integrity by preventing loosening tendencies and providing the structure's resilience against fatigue. The bolt pretension is very important for the bolted

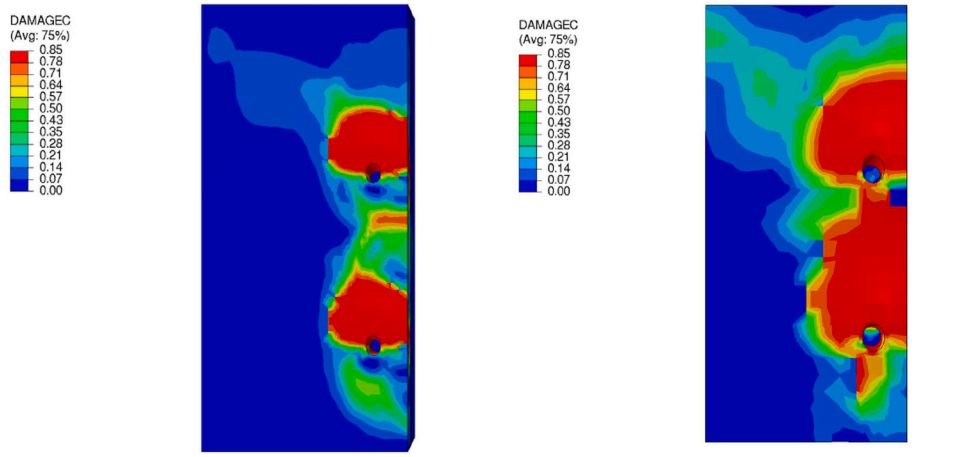

Fig. 14. Failure modes of FE Model.

shear connector design. In the experimental study the magnitude of this preload was obtained using a torque spanner. Fig. 16 and Table 7 showed the effect of the bolt pretension values on the behaviour of the bolted shear connection. From Fig. 16, the bolt pretension did not have any effect on the structure's ultimate load, and they were almost the same as listed in Table 7. Notably, the primary disparity among slip curves corresponding to diverse preloads in the finite element model primarily manifests during the initial stage. As the value of the bolt pretension increased, the value of the load raised when the stiffness of the structure was changed. This phenomenon is rooted in the fact that the increase in bolt preload leads to an increase in friction between the concrete and the steel beam. As a result, the structure exhibits greater slip resistance during the initial phase of loading.

4.6.3. *Effect of the nut diameter*

In contrast to the bolted shear connectors examined in previous literature [28-30], the new shear connectors under scrutiny employ a distinct configuration—a specially designed elongated nut embedded within the concrete slab, serving as a connection point for the bolt. This is different with the traditional short nut design results in an expanded contact surface between the shear connector and the concrete. The purpose of this design alteration is twofold: mitigating stress concentration within the concrete and safeguarding it against potential crushing, thereby augmenting the specimen's resistance. Thus, the dimensions of this elongated nut emerge as a pivotal parameter for this connector. Fig. 17 and Table 8 shows the numerical results of the specimens with different nut diameters. From Fig. 17 and Table 8, the ultimate load-bearing capacity of the structure is increased with the nut diameter induces. When transitioning from a 28 mm nut diameter to 30 mm, 32 mm, and 34 mm, the ultimate load capacity experienced successive increments of 33.65 kN, 40.41 kN, and 36.07 kN, respectively. This observation serves to validate the efficacy of employing an elongated nut as opposed to the conventional alternative, as evident from the concrete damage prevention achieved. Furthermore, the nut diameter influences the shear connectors' stiffness. As the nut diameter increases from 28 mm to 34 mm, the shear connectors' stiffness has a proportional increase of 9.76 %.

4.6.4. *Effect of the bolt diameter*

The influence of the bolt diameter on the push-out experiment was shown in Fig. 18. As shown in Table 9, for the new bolt connector, the ultimate load and shear stiffness increase slightly with the bolt diameter from 20 mm to 26 mm. The ultimate load capacity of the structure exhibits an increment of 14.52 %. As shown in Table 9, the structural

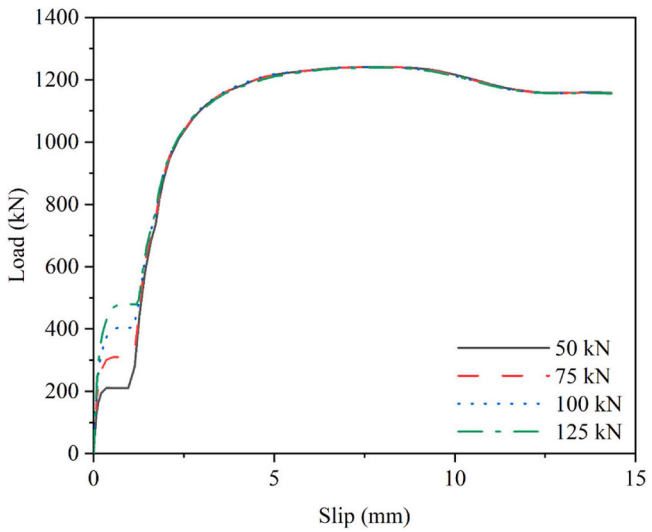

Fig. 16. Effect of bolt pretension for novel bolted shear connectors.

Table 7
Effect of the bolt pretension for novel bolted shear connectors.

Bolt pretension (kN)	Ultimate load (kN)	Stiffness of shear connector k (kN/mm)
50	1241.25	106.49
75	1241.82	96.32
100	1240.83	85.99
125	1239.12	86.31

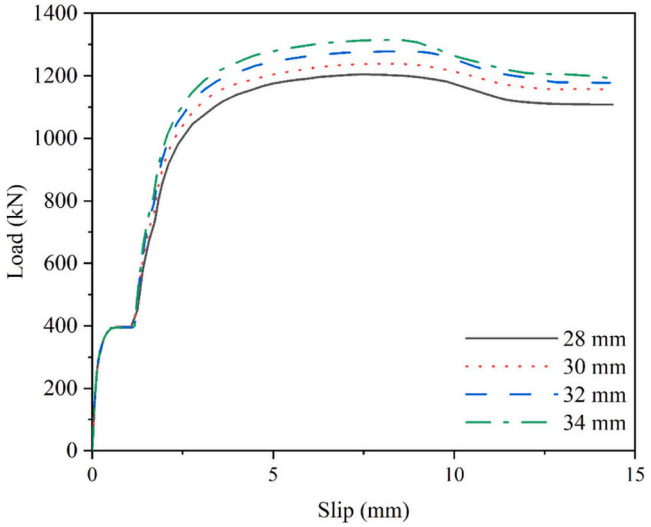

Fig. 17. Effect of diameter of nut for novel bolted shear connectors.

Table 8
Parametric study results: effect of diameter of nut for novel bolted shear connector.

Diameter of nut (mm)	Ultimate load (kN)	Stiffness of shear connector k (kN/mm)
28	1204.78	222.19
30	1238.43	232.00
32	1278.84	243.79
34	1314.91	254.31

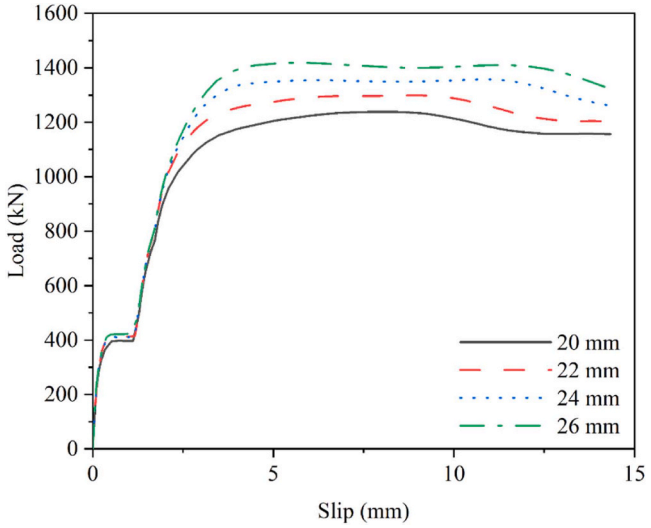

Fig. 18. Effect of diameter of the shear connectors for novel bolted shear connectors.

Table 9
Effect of dimeter of shear connectors for novel bolted shear connector.

Diameter of shear connectors (mm)	Ultimate load (kN)	Stiffness of shear connector k (kN/mm)
20	1238.43	232.00
22	1298.54	249.53
24	1357.59	266.76
26	1418.27	284.45

stiffness increased with the bolt diameter.

4.6.5. *Effect of concrete strength*

Fig. 19 illustrated the effect of concrete strength on the structure with new bolted shear connectors. From the figure, the load capacity of the push out specimen using new bolted shear connectors increased with the concrete strength. The results are consistent with existing studies by PavloviA et al. [13] and Pathirana et al. [11]. As shown in Section 3, the experimental results showed that the ultimate load capacity of the specimens was mainly dominated by the strength of the concrete and the failure pattern was concrete crushing. As concrete strength escalated, the structure demonstrated an increased ability to withstand external loads before succumbing to concrete deformation around the bolts. This, in turn, facilitated an optimization of the structure's ultimate load-bearing capacity. From Figs. 19 and 20, the influence of the concrete strength exhibited a similar trend between new bolted shear connectors and conventional welded studs. Both the shear stiffness and the ultimate load-bearing capacity increased with the concrete strength. For the specimens with these two types of connectors, the ultimate load-bearing capacity of the new bolted shear connector was much larger than that of conventional welded studs. Moreover, from Tables 10 and 11, the shear stiffness of the new connectors was comparatively higher than that of the welded studs when the bolt clearance was ignored.

5. Conclusions

The numerical and experimental studies on the local behaviours of novel bolted shear connectors have been conducted in this paper and the results were compared with that of a conventional welded shear connector. The FE model was established and validated using experimental results, and the parametric studies were conducted using the validated model. The effect of the concrete strength, the shear connector diameter, the bolt pretension, the gap between the bolt hole and bolt,

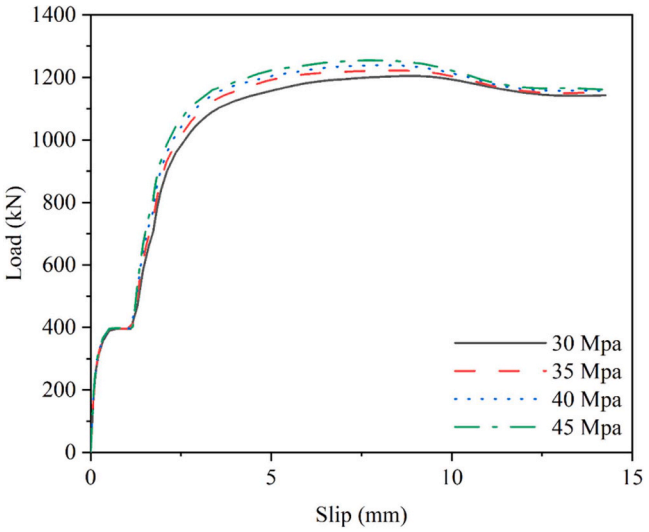

Fig. 19. Effect of concrete strength for novel bolted shear connectors.

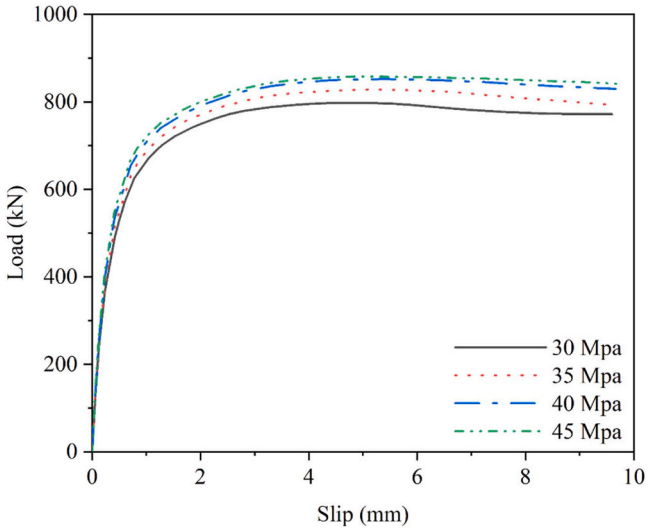

Fig. 20. Effect of concrete strength for welded studs.

Table 10
Parametric study results: effect of concrete strength for novel bolted shear connector.

Concrete strength	Ultimate load (kN)	Stiffness of shear connector k (kN/mm)
C30	1204.79	222.19
C35	1221.98	227.20
C40	1238.43	232.00
C45	1254.32	236.64

Table 11
Parametric study results: effect of concrete strength for welded studs.

Concrete strength	Ultimate load (kN)	Stiffness of shear connector
C30	798.10	149.64
C35	827.96	156.93
C40	852.18	163.25
C45	858.08	165.67

and the nut diameter on the local behaviours of shear connectors was discussed. The following conclusions are obtained through experiments and numerical simulations:

1. From the experimental results, the novel shear connection has excellent mechanical properties. Compared with the conventional studs, the ultimate load capacity and ductility of the new bolted shear connection are increased by 46.23 % and 50.22 %, respectively. The overall shear stiffness of the new bolted connection is 7 % higher than that of the conventional connection. Moreover the initial stiffness of the new shear connection was lower compared to that of the conventional connection due to the bolt clearance.
2. From numerical results, the strength of concrete has a slight effect on the performance of the shear connection. The ultimate load capacity of novel and conventional shear connectors increased by 4.1 % and 7.5 %, respectively, when the concrete strength increased from 30 MPa to 45 MPa. The failure mode of specimens with different shear connections was the localized crushing of concrete near the connectors. The surface area of the nut embedded in the concrete slab helped to reduce the concentrated forces that led to longitudinal cracking in the concrete slab, thereby delaying concrete cracking and increasing the load capacity. Compared with the conventional shear connection, the ultimate load capacity of the new bolted connection increased by 45.3 % for 40 MPa concrete specimens.

3. From numerical results, the ultimate load-carrying capacity of the structure is significantly affected by the diameters of the long-tube nut and bolt. The ultimate load-carrying capacity of the structure increased by 9.76 % when the nut diameter increased by 21.4 %. 14.5 % increase in the bolt diameter results 14.5 % increase in the capacity.

CRediT authorship contribution statement

Peng Dong: Data curation. **Xinqun Zhu:** Conceptualization, Methodology, Supervision, Writing – review & editing, Funding acquisition. **Jun Li:** Supervision, Writing – review & editing. **Chenguang Li:** Conceptualization, Formal analysis, Methodology, Software, Validation, Writing – original draft, Writing – review & editing.

Declaration of Competing Interest

The authors declare no known competing interest exist.

Acknowledgements

This study was supported by the Australia Research Council (ARC) Discovery Project (DP) No.: 23010806.

References

[1] Galambos TV. Recent research and design developments in steel and composite steel–concrete structures in USA. J Constr Steel Res 2000;55(1):289–303.
[2] Shamass R, Cashell KA. Behaviour of composite beams made using high strength steel. Structures 2017;12:88–101.
[3] de Lima Araújo D, Reis Sales MW, de Paulo SM, de Cresce El Debs AH. Headed steel stud connectors for composite steel beams with precast hollow-core slabs with structural topping. Eng Struct 2016;107:135–50.
[4] He J, Liu Y, Pei B. Experimental study of the steel-concrete connection in hybrid cable-stayed bridges. J Perform Constr Facil 2014;28(3):559–70.
[5] Suwaed ASH, He J, Vasdravellis G. Experimental and numerical evaluation of a welded demountable shear connector through horizontal pushout tests. J Struct Eng ASCE 2022;148(2):0003269.
[6] Suwaed ASH, Karavasilis TL. Removable shear connector for steel-concrete composite bridges. Steel Compos Struct 2018;29(1):107–23.
[7] Brambilla G, Lavagna M, Vasdravellis G, Castiglioni CA. Environmental benefits arising from demountable steel-concrete composite floor systems in buildings. Resour, Conserv Recycl 2019;141:133–42.
[8] Hosseini SM, Mashiri F, Mirza O. Research and developments on strength and durability prediction of composite beams utilising bolted shear connectors (Review). Eng Fail Anal 2020;117:104790.
[9] Liu XY, Bi ZJ, Hu JY, Hao HS, Lin ZS, Li HW, et al. Bolted shear connectors in steel-concrete composite structures: shear behaviour. Structures 2023;58:105524.
[10] Ataei A, Zeynalian M. A study on structural performance of deconstructable bolted shear connectors in composite beams. Structures 2021;29:519–33.
[11] Pathirana SW, Uy B, Mirza O, Zhu X. Strengthening of existing composite steel-concrete beams utilising bolted shear connectors and welded studs. J Constr Steel Res 2015;114:417–30.
[12] Hawkins NM. Strength in shear and tension of cast-in-place anchor bolts. Am Concr Inst Symp 1987;103:233–56.
[13] PavloviA M, MarkoviA Z, VeljkoviA M, BuAevac D. Bolted shear connectors vs. headed studs behaviour in push-out tests. J Constr Steel Res 2013;88:134–49.
[14] Kwon G, Engelhardt MD, Klingner RE. Behavior of post-installed shear connectors under static and fatigue loading. J Constr Steel Res 2010;66(4):532–41.
[15] Tzouka E, Karavasilis T, Kashani MM, Afshan S. Finite element modelling of push-out tests for novel locking nut shear connectors. Structures 2021;33:1020–32.
[16] He J, Suwaed ASH, Vasdravellis G. Horizontal pushout tests and parametric analyses of a locking-bolt demountable shear connector. Structures 2022;35:667–83.
[17] He J, Suwaed ASH, Vasdravellis G, Wang SH. Standard pushout tests and design rules for a bolted-welded hybrid demountable shear connector. J Struct Eng ASCE 2022;148(8):04022097.
[18] EN 1994–1-1: 2004. Eurocode 4: design of composite steel and concrete structures—part 1.1: general rules and rules for buildings.
[19] GB/T 50081–20192019. Standard for test methods of concrete physical and mechanical properties.
[20] GB/T 50017- 20172017. Standard for design of steel structures.
[21] Simulia, D.C.S. (2011). Abaqus 6.11 analysis user's manual.
[22] GB 50010–20152015. Code for design of concrete structures.
[23] Pathirana SW, Uy B, Mirza O, Zhu X. Bolted and welded connectors for the rehabilitation of composite beams. J Constr Steel Res 2016;125:61–73.
[24] Liang QQ, Uy B, Bradford MA, Ronagh HR. Ultimate strength of continuous composite beams in combined bending and shear. J Constr Steel Res 2004;60(8):1109–28.
[25] Loqman N, Safiee NA, Bakar NA, Nasir NAM. Structural behavior of steel-concrete composite beam using bolted shear connectors: a review. MATEC Web Conf 2018;203:06010.
[26] Liu X, Bradford MA, Chen Q-J, Ban H. Finite element modelling of steel–concrete composite beams with high-strength friction-grip bolt shear connectors. Finite Elem Anal Des 2016;108:54–65.
[27] Liu X, Bradford MA, Lee MSS. Behavior of high-strength friction-grip bolted shear connectors in sustainable composite beams. J Struct Eng ASCE 2015;141(6).
[28] Ataei A, Bradford MA, Liu X. Experimental study of composite beams having a precast geopolymer concrete slab and deconstructable bolted shear connectors. Eng Struct 2016;114:1–13.
[29] Chiniforush AA, Ataei A, Bradford MA. Experimental study of deconstructable bolt shear connectors subjected to cyclic loading. J Constr Steel Res 2021;183:106741.
[30] Hirashima T, Hamada N, Ozaki F, Ave T, Uesugi H. Experimental study on shear deformation behaviour of high strength bolts at elevated temperature. J Struct Constr Eng 2007;621:175–80.